

# Mathematical Models of Fingerprint Image On the Basis of Lines Description

Vladimir Gudkov

Department of Applied Mathematics

Chelyabinsk State University, Chelyabinsk, Russia

[diana@sonda.ru](mailto:diana@sonda.ru)

## Abstract

This paper presents a mathematical models of fingerprint based on the lines as topological vectors and ridge count. They are stored in the template with the list of minutiae. Templates are used to identify the fingerprint.

**Keywords:** *Fingerprint, minutiae, topology, ridge count, template, vector.*

## 1. INTRODUCTION

Fingerprint images (FI) identification is realized on the basis of the templates, containing the pattern features. Their basis is minutiae description in the form of beginnings and endings, junctions and bifurcation of lines [5-7]. They can be detected by gray image, though in the process of template creation they are guided by the lines skeleton [1, 5] (figure 1).

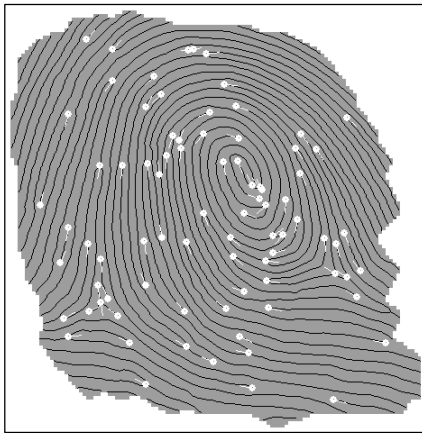


**Figure 1.** Skeleton and minutiae

Image mathematical model should depend on necessary and sufficient quantity of features [1]. Minutiae and ridge count between minutiae are reputed as informative in dactyloscopy [5]. However they do not exhaust all the great number of mathematical models, used in Biometrics for automatic proof of pattern individuality [3–6]. Each of such models is focused to increase the identification accuracy, but any better, free from defect model is not known [5]. For example, classical ridge count, which should be counted along the straight line due to criminalistics, does not stand up to criticism in the area of considerable curvature of pattern lines and in the area of loops, deltas and whorls [4, 7].

## 2. IMAGE TEMPLATE

The templates as a set of FI features are varied at different software producers. Some templates formats are limited in minutiae quantity [5]. Some features of templates are irrelevant but it is possible to indicate their common property: the templates have features, being some metrics for minutiae. These are ridge count between minutiae and topological vector for minutiae [5-7]. In paper an image template is synthesized in the form of

$$\Gamma : F_0^{(m)} \rightarrow \{L_m, L_l, L_r\}, \quad (1)$$

where  $F_0^{(m)} = [f_0^{(m)}(x, y)]$  – image skeleton (figure 1);  $L_m$  – minutiae list;  $L_l$  – topological vectors list for lines;  $L_r$  – ridge count vectors list for lines. Let's introduce some definitions.

**Definition 1.** The skeleton of the line is simple circuit  $\langle u, v \rangle$  with nodes  $u$  and  $v$  in 8- adjacency, which is near geometrical center of the line, at that there are two adjacent nodes  $p_2$  and  $p_3$  for each node  $p_1 \in \langle u, v \rangle$ , at that the nodes  $p_2$  and  $p_3$  non-adjacent.

**Definition 2.** Ending is such node  $p_1$  of the skeleton, that there is one adjacent node  $p_2$  for the node  $p_1$ .

**Definition 3.** Bifurcation is such node  $p_1$  of the skeleton, that there are three adjacent nodes  $p_2$ ,  $p_3$  and  $p_4$  for the node  $p_1$ , at that any two nodes from the multitude  $\{p_2, p_3, p_4\}$  are non-adjacent in pairs.

Elements of both topological vector and ridge count vector for line are determined with endings and bifurcations, which are read from the skeleton nodes as nodes of graph. These vectors are derivative from minutiae. However all these vectors characterize not the area of separately selected point, but common properties of point's multitude or line segment. In spite of the fact that the lists  $L_l$  and  $L_r$  characterize FI differently, they are alike in that they represent description for all pattern lines, but not for all the lines points, which can be much more in number. This interesting peculiarity allows synthesizing compact templates.

### 2.1. Minutiae list

Let  $M_i$  – is minutiae which is indexed to number  $i$ . The minutiae list  $L_m$  is in the following form

$$L_m = \{M_i = \{(x_i, y_i), \alpha_i, t_i, v_i, \theta_i, p_i, h_i\} | i \in 1..n_1\}, \quad (2)$$

where  $|L_m| = n_1$  – cardinal number;  $(x_i, y_i)$ ,  $\alpha_i$ ,  $t_i$ ,  $v_i$ ,  $\theta_i$ ,  $p_i$ ,  $h_i$  – coordinates, direction and type of minutiae, as well as value and direction of curvature, probability and density of lines about minutiae. Minutiae are detected in the informative area (on the figure 1 FI informative area is darkened, but the skeleton is black) [3, 4]. They are not detected on the edge of informative area.

Coordinates  $(x_i, y_i)$  of minutiae  $M_i$  are determined with coordinates of skeleton node [1]. Direction  $\alpha_i$  like the angle is determined with circuit of skeleton nodes for ending and tree circuits for bifurcation [2, 5]. Type  $t_i \in \{0,1\}$  is determined with skeleton nodes valence like the nodes of graph [2], where 0 – bifurcation and 1 – ending. Coordinates  $(x_i, y_i)$ , direction  $\alpha_i$  and type  $t_i$  are the basic parameters  $M_i$  [5-7].

Value  $v_i$  and direction  $\theta_i$  of the curvature are determined by lines direction difference in the neighborhood  $\varepsilon$  of minutiae  $M_i$  [3, 4]. Probability  $p_i$  is calculated as the ratio of the average value of image quality rating in the neighborhood  $\varepsilon$  to the best quality rating in the FI informative area [3]. Lines density  $h_i$  is calculated as the average quantity of lines, located into the neighborhood  $\varepsilon$  on the straight line traced transversely to lines [3-5]. A value of neighborhood  $\varepsilon$  is assigned.

## 2.2. Topological vectors list

Topological vectors list for lines  $L_l$  is found on the basis of minutia list  $L_m$ , skeleton as the matrix  $F_0^{(m)}$  and other auxiliary matrixes, elements of which reflect FI local features. These matrixes are formed in the pyramid, which present data informational layers, distributed among the hierarchy [1]. Topological vectors list for lines is synthesized on the basis of all the nodes of skeleton, excluding minutiae nodes, and written in the form of

$$L_l = \{V_i = \{(e_j, n_j, l_j)\} | i \in 1..n_2, j \in 1..m_t\}, \quad (3)$$

where  $V_i$  – topological vector for skeleton nodes cluster;  $|L_l| = n_2$  – cardinal number and  $n_2 > n_1$ ;  $i$  – index like the number of topological vector;  $j$  – number of link in topological vector;  $e_j$  – event, and  $l_j$  – length of link, formed with minutiae with number  $n_j$ ;  $m_t$  – quantity of links taking into account central line in the form of

$$m_t = 4m + 2. \quad (4)$$

Let's dwell on the procedure of list synthesis.

In the FI informative area the lines are marked out and an image formalized as skeleton is formed. Two types of minutiae are detected on skeleton: endings and bifurcations (figure 1). Minutiae directions (angle) point to the area of lines number increase [5]. It is parallel to the tangent to papillary line in the small neighborhood of minutiae  $M_i$ . Every minutia is numbered and described with coordinates, direction, type, value and direction of curvature, probability and density (2).

Further from each minutia we draw projections to the right and to the left transversely to the direction vector of the minutiae onto

adjacent lines and fix the projections. On the figure 2 the projections are shown with dotted lines, and two corresponding nodes of skeleton on the lines 1 and 2 are painted over.

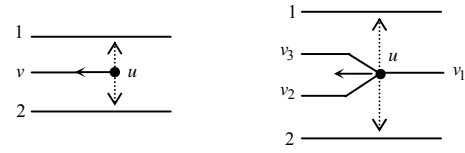


Figure 2. Projections for ending and bifurcation

Let's choose the skeleton node  $p_i$  (not the minutiae) and pass across its coordinates  $(x_i, y_i)$  the section to the right and to the left at a distance of  $m$  lines transversely to the tangent to lines being crossed and enumerate on gyrate the dissected lines (hereinafter 'links'), which turn clockwise. The section passes and traces the lines curvature [3]. The section depth  $m$  is varied from one up to eight lines to the right and the same to the left. One line in the section forms two links. The quantity of links in topological vector is calculated according to (4).

Topological vector is determined by the section. To do this we'll follow the move of every link by turns on each link, not leaving it and beginning from the section till meeting another minutiae, located on the link, or a minutiae projection, located on an adjacent line to the right or to the left of the link. At that on the links detected the following possible events, shown on the figure 3 and represented in a binary code:

**1101** – an ending projection is detected on the link, which locates to the right of the link in the course of tracing the link, the direction vector of the ending is directed contrariwise to the link course;

**1001** – an ending projection is detected on the link, which locates to the right of the link in the course of tracing the link, the direction vector of the ending is directed along the link course;

**1110** – an ending projection is detected on the link, which locates to the left of the link in the course of tracing the link, the direction vector of the ending is directed contrariwise to the link course;

**1010** – an ending projection is detected on the link, which locates to the left of the link in the course of tracing the link, the direction vector of the ending is directed along the link course;

**0101** – a bifurcation projection is detected on the link, which locates to the right of the link in the course of tracing the link, the direction vector of the bifurcation is directed contrariwise to the link course;

**0001** – a bifurcation projection is detected on the link, which locates to the right of the link in the course of tracing the link, the direction vector of the bifurcation is directed along the link course;

**0110** – a bifurcation projection is detected on the link, which locates to the left of the link in the course of tracing the link, the direction vector of the bifurcation is directed contrariwise to the link course;

**0010** – a bifurcation projection is detected on the link, which locates to the left of the link in the course of tracing the link, the direction vector of the bifurcation is directed along the link course;

**0011** – a bifurcation is detected on the link, the direction vector of the bifurcation is directed along the link course;

**0111** – a bifurcation is detected on the link, formed with the line, the tangent to which forms a minimum angle at the bifurcation direction vector rotating on the link counterclockwise;

**1011** – a bifurcation is detected on the link, formed with the line, the tangent to which forms a minimum angle at the bifurcation direction vector rotating on the link clockwise;

**1111** – an ending is detected on the link, the direction vector of the ending is directed contrariwise to the link course;

**1100** – a minutia or a minutia projection is not detected and the link on the line is close.

**0000** – a minutia or a minutia projection is not detected and the link terminates at a papillary pattern or non-informative area edge;

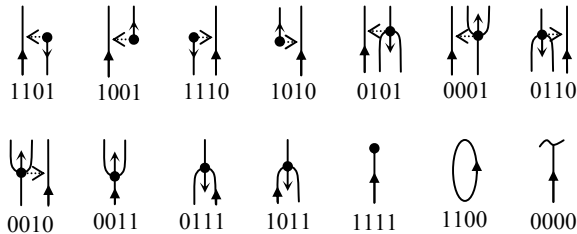


**Figure 3.** Events

Minutiae' number initiated the event is associated with the event as the number (14 in sum) detected on the link. The event is tied to the link number. For 0000 and 1100 events the numbers of minutiae are absent. Enumerated set of links with formed events and minutiae' numbers is the **basic topological vector** (economical). The event and minutiae' number form ordered pair  $(e_j, n_j)$ . The event is amplified with link length from the section up to the position, in which the event is detected. **Enlarged topological vector** is formed in such way. The event, minutiae' number and length of the link form an ordered triplet  $(e_j, n_j, l_j)$ . For 0000 and 1100 events the links lengths can describe the informative areas without minutiae! The lengths of links, broken on FI edge, are stable in the meaning that they are not shortened in case of fool rolling of the finger [3].

Bit location in the event determines minutiae type, its direction regarding the link course, its location regarding the link etc. Events allow on-the-fly compare the **basic topological vectors** and speed up the identification procedure [3].

Topological vectors are built for every node of the skeleton  $p_i$  (excepting minutiae). The section divides the lines into the links, numbered on gyrate, turning clockwise. On the figure 4 in the section for the node A of skeleton line, ending in 19, the links are enumerated as 0–17. Topological vector of the node A is shown in the table 1. On the figure 5 in the section for the node B of the skeleton line, which is locked in bifurcation 19, the links are enumerated as 0–17. Topological vector of the node B is shown in the table 2. The sections are shown with dotted line, and the figures represent usual mutation [3] of ending 19 into bifurcation 19 (because of the dirty skin). Per se the nodes A and B of the skeleton are the same.

The start of links numbering in the section for the nodes A and B (link № 0) is insignificant, as since in case of FI turn over the mirror of links numbers in the section is formed, which is easy recognized and taken into account at FI identification. By analogy with the game «Puzzle» assembling is realized by the way of joining of corresponding connectors. At the section depth  $m = 4$  18 links  $m_i = 18$  for the line are formed according to (4).

The quantity of topological vectors is enumerable. At the foot of the figure 4 with two-forked dotted arrow is shown the zone, located between minutiae 19 and 25, within the bounds of which for the point A at its displacement on the skeleton the same **basic**

**topological vector** is synthesized. The similar zone between minutiae 19 and 25 for the point B is shown at the foot of the figure 5. Topological vectors with equal **basic topological vectors** are integrated into one [3]. At that their quantity is reduced by dozens of times from the value  $n_2 < 1000$  according to (3) to the value  $n_1 < 100$  according to (2). Vector  $V_i$  automatically characterizes the line segment, but not the minutiae. The image deformation, especially linear, practically doesn't have any effect upon the content of the **basic topological vector**. Therefore the vector is named as topological [3, 6, 7].

Here on the list formation (3) is finished.

**Table 1.** Topological vector for A

Number	Event	Index	Length
0	1110	22	$l_0$
1	1111	19	$l_1$
2	1110	19	$l_2$
3	1111	22	$l_3$
4	0001	21	$l_4$
5	1101	19	$l_5$
6	1010	24	$l_6$
7	0010	25	$l_7$
8	0011	21	$l_8$
9	1111	23	$l_9$
10	1010	26	$l_{10}$
11	0011	25	$l_{11}$
12	0010	21	$l_{12}$
13	1010	20	$l_{13}$
14	1111	27	$l_{14}$
15	0001	25	$l_{15}$
16	0000	–	–
17	1001	20	$l_{17}$

**Table 2.** Topological vector for B

Number	Event	Index	Length
0	1110	22	$l_0$
1	1011	19	$l_1$
2	0111	19	$l_2$
3	1111	22	$l_3$
4	0001	21	$l_4$
5	0101	19	$l_5$
6	0110	19	$l_6$
7	0010	25	$l_7$
8	0011	21	$l_8$
9	1111	23	$l_9$
10	1010	26	$l_{10}$
11	0011	25	$l_{11}$
12	0010	21	$l_{12}$
13	1010	20	$l_{13}$
14	1111	27	$l_{14}$
15	0001	25	$l_{15}$
16	0000	–	–
17	1001	20	$l_{17}$

Comparative analysis of [3] and [6] show, that [3] has a series of advantages. Firstly, the section is built along the curved line, which traces curvature direction of the crossed lines. Secondly, at the events calculation the projection of minutiae is used, that result in prevention of the information loss. Thirdly, the links enumerating is turning along the gyrate without links omission.

Fourthly, at integration it is possible to choose topological vector with maximum value of minimal length of link (3). This raises stability and comprehension of mathematical model.

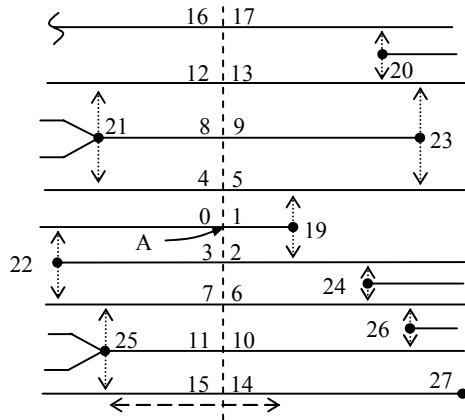


Figure 4. Section for line with ending

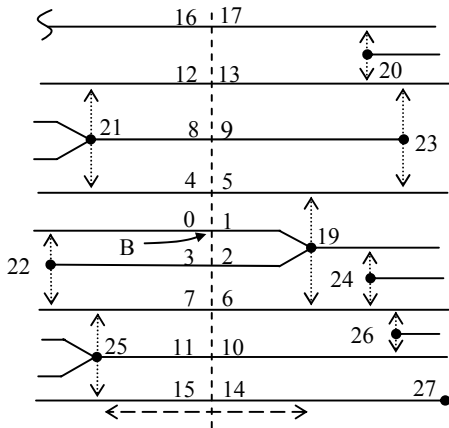


Figure 5. Section for line with bifurcation

### 2.3. Ridge count vectors list

In dactyloscopy the ridge count is the base for evidence of fingerprint identity in a Court. It should be calculated as the quantity of lines, placed on the straight line between two minutiae. In electron systems for one minutia  $M_i$ , as a rule, some similar values are determined.

According to [5] from the list  $L_m$  regular minutia  $M_i$  is chosen and taken as a center of the scanning ray rotation, the initial location of which coincides with the vector direction  $\theta_i \in M_i$  according to (2). The image is scanned, rotating the scanning ray. At the meeting of a ray with  $M_k \in L_m$  the ordered pair  $(r_j, n_j)$  is formed, where  $n_j = k -$  number of minutiae  $M_k$  and  $k \neq i$ ;  $r_j$  – ridge count between  $M_i$  and  $M_k$ ;  $j$  – number of link as the quantity of minutiae met by a ray. The number of such pairs is not more than  $n_1 - 1$ .

These actions repeat  $\forall M_i \in L_m, i \in 1..n_1$ . Geometrical characteristics connected with ordered pair and served as derivative from the minutiae and the scanning angle parameters,

are redundant for the model and calculated at the time of identification. In the templates the links quantity for  $M_i$ , as a rule, is limited, and the links are clustered as quadrants or octants, oriented according to  $\theta_i \in M_i$  of the co-ordinates.

There are three main disadvantages of ridge count, mentioned in [4-6]. Firstly, a value  $r_j$  is unstable as since in case of mutation of the ending into bifurcation or vice versa the ridge count value is changed. Secondly, in the area of loops, deltas, whirls and considerable curvature of lines, the ridge count is doubtful because of the straight line measuring mechanism. Thirdly, clustering of ridge count values in quadrants or octants results in appearance of boundary effect, which realized in the fact that, minutiae can pass through the limits of plane partition into regions. This increases the identification mistakes a lot.

To solve mentioned defects, it is suggested the list of ridge count vectors for lines, which is synthesized on the basis of all the nodes of skeleton  $F_0^{(m)}$ , excluding minutiae nodes, of some auxiliary matrixes of the pyramid [1] and minutiae list  $L_m$  in the form of

$$L_r = \{R_i = \{(r_j, n_j) | i \in 1..n_3, j \in 1..n_4\}, \quad (5)$$

where  $R_i$  – is a vector of ridge count for the nodes group of the skeleton as ordered by index  $j$  set of ordered pairs  $(r_j, n_j)$ ;  $|L_r| = n_3$  – cardinal number and  $n_3 > n_1$ ;  $i$  – index as a number of vector;  $j$  – link number in a vector;  $n_4$  – links quantity in a vector and  $n_4 < n_1$ ;  $r_j$  – ridge count value, and  $n_j$  – minutiae number as in (2) on a link  $j$ .

Let's dwell on the sequence of operations being carried out.

In the informative area of FI we choose lines and form skeleton, using which we detect two types of minutiae: endings and bifurcation [5]. Minutiae direction (angle) point to the area of lines number increase (figure 2). It is parallel to the tangent of papillary line in small area around the minutia  $M_i$ . Each minutia is numbered and described with coordinates, direction and type, as well as curvature value and direction, probability and density of the lines in the neighborhood  $\varepsilon$  of the minutia (2).

Let's choose the skeleton node  $p_g$  (but not the minutiae) and take it for the rotation center of the scanning ray, initial direction of which coincides with the skeleton line direction. The image is scanned, rotating the scanning ray. At the meeting of a ray with  $M_k \in L_m$  the ordered pair  $(r_j, n_j)$  is formed, where  $n_j = k -$  number of minutiae  $M_k$ ;  $r_j$  – ridge count between  $p_g$  and  $M_k$ ;  $j$  – number of link as the quantity of minutiae met by a ray. As a result of one rotation of a ray **ridge count vector**  $R_g = \{(r_j, n_j) | j \in 1..n_1\}$  is formed as enumerated by index  $j$  set of ordered pairs  $(r_j, n_j)$ . These operations are represented for all skeleton nodes (excepting minutiae). The links are closed as a ring and the enumeration can be renewed with changing of the initial direction of a scanning ray, for example  $R_g^s = \{(r_l, n_l) | l \in 1..n_1\}$ , where the number of link is  $l = (j + s) \bmod (n_1 + 1)$ . In that case for the node  $p_g$  on the basis of vector  $R_g$  it is possible taking into account links closing as a ring to synthesize  $|R_g^s | s \in 1..n_1 | = n_1$  **equivalent vectors of ridge count**.

The final set of ridge count vectors is formed for the skeleton. **Ridge count vectors**, for which it is possible to synthesize the similar **equivalent vectors of ridge count**, integrate into one [4]. Join means a choice, for example at random one of integrated vectors and placing it into the list of ridge count vectors  $L_r = \{R_i | i \in 1..n_3\}$  according to (5). The quantity of vectors is reduced by one-two order. A vector  $R_i$  for the image is unique and automatically characterizes the line segment.

Here on the list building (5) is finished.

There are following advantages. Firstly, ridge count on the one end is closed to the node of skeleton, which is not prone to minutiae mutations, that increases the stability of the ridge count value  $r_j$ . Secondly, the lines in the area of loops, deltas, whirls and essential curvature are automatically divided with vectors  $R_i$  for short intervals that allow detailing differently the FI conception and reducing mistakes of identification. The quantity of links in the vector can be limited, for example, on the ray length criterion.

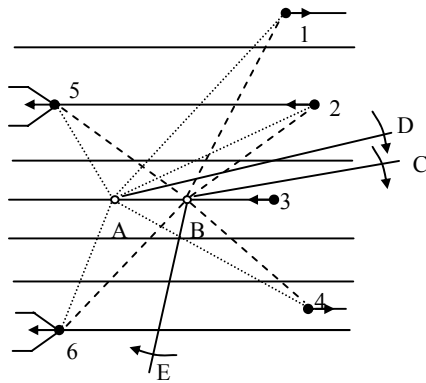


Figure 6. Ridge count of a line

On the figure 6 the node B is chosen as a center of scanning ray BC rotation. At the scanning ray rotating clockwise round the node B with indicated on the figure 6 initial location, the scanning ray will meet with minutiae 3,4,6,5,1,2 in turn. If ridge count determined with quantity of crossed lines along the ways, shown with long-dotted line, than for the sequence of met minutiae ridge count values 0,2,2,1,3,1 are generated. This represents with ordered set of pairs (0,3),(2,4),(2,6),(1,5),(3,1),(1,2), which forms ridge count vector for the node B. At another initial location of the scanning ray, for example ray BE, another set of pairs (2,6),(1,5),(3,1),(1,2),(0,3),(2,4) is determined, which in case of closing into the ring identified with source set of pairs (0,3),(2,4),(2,6),(1,5),(3,1),(1,2). Actually, for the set of ordered pairs of the node B there are 6 equivalent vectors of ridge count.

If the node A is chosen with the help of scanning ray AD, which is rotating clockwise, than the ordered set of pairs (0,3),(2,4),(2,6),(1,5),(3,1),(1,2) is formed. It coincides with one of equivalent vectors of ridge count for the node B (independently of the initial direction of the ray AD). Vectors of ridge count for the node A and nodes B are integrated into one.

### 3. CONCLUSION

In this paper we suggested mathematical model of FI on the basis of topological vectors for the lines (3), which is stored in the template (1). Topological vectors form linked graph with a high

level of redundancy. This allows connecting sub graphs [3] of fragmentary latents of fingerprints. List  $L_l$  according to (3) can be represented in economic format (without links lengths). Minutiae mutation don't change the links enumerating and minutiae enumeration queue (tables 1, 2), that increases stability of mathematical model.

Topological vectors stability is additionally increased by integrating **basic topological vectors** into one corresponding **enlarged topological vector**, where the minimum length of link is maximal [3].

We suggested mathematical model of FI on the basis of **ridge count vectors** for lines (5), which demonstrate raised stability at calculating of ridge count values. Additionally the lines in the area of loops, deltas, whirls and essential curvature are automatically divided with ridge count vectors in more detail independently from minutiae location that increases stability of mathematical model as well.

An image template according to (1) as a set  $\{L_m, L_l, L_r\}$  consists of lists  $L_l$  according to (3) and  $L_r$  according to (5) which are mutually complementary, for them minutiae list is the determining one according to (2). The lists  $L_l$  and  $L_r$  are essentially different and don't replace each other, but one of these lists can be excluded from this template. Moreover topological vectors can be stored in enlarged or economic variant (without links lengths). This allows optimizing required memory capacity for the template storage.

### 4. REFERENCES

1. Gonzales, R. Digital processing of the images / R. Gonzales, R. Woods; translation from English; the editor P. Chochia – M.: Techno sphere, 2006. – 1072 p.
2. Novikov, F. Discrete Mathematics for programmers: manual / F. Novikov. – St. Petersburg: Piter, 2001. – 304 p.
3. Patent 2321057 Russian Federation, Int. Cl. G 06 K 9/52, A 61 B 5/117. The Method of Papillary Pattern Print Coding / V. Gudkov – № 2006142831/09; Field: Dec. 04, 2006; Date of patent: Mar. 27, 2008; Bull. № 9. – 13 p.
4. Favourable decision on application Russian federation, Int. Cl. G 06 K 9/00. The Method of Papillary Pattern Print Coding / V. Gudkov, A. Bokov, A. Mosunov. – № 2007118575/09; Field: May. 18, 2007; Date of patent: Nov. 27. 2008; Bull. № 33. – 13 p.
5. Maltoni, D. Handbook of fingerprint recognition / D. Maltoni, D. Maio, A.K. Jain. – New York: Springer-Verlag, 2003. – 348 p.
6. Pat. 5631971 USA, Int. Cl. G 06 K 9/00. Vector based topological fingerprint matching / M.K. Sparrow (Winchester). – Field: Jul. 15, 1994; Date of patent: May. 20, 1997; U.S.Cl. 382/125. – 17 p.
7. Sparrow, M.K. A topological approach to the matching of single fingerprints: development of algorithms for use on latent finger marks / M.K. Sparrow, P.J. Sparrow // US dep. comer. nat. bur. stand. spec. pub. – 1985. – № 500–126. – 61 p.

### About the author

Vladimir Gudkov is a doctor at Chelyabinsk State University, Department of Applied Mathematics. His contact e-mail is diana@sonda.ru.